UNCLASSIFIED

CENTRAL RESEARCH LIBRARY
DOCUMENT COLLECTION

MARTIN MARIETTA ENERGY SYSTEMS LIBRARIES
3 4456 0352739 7

ORNL 933
Series B
PHYSICS

TRANSPORT PARAMETERS FOR THERMAL NEUTRONS IN WATER

FRANCIS J. SISK

CENTRAL RESEARCH LIBRARY
DOCUMENT COLLECTION

LIBRARY LOAN COPY

DO NOT TRANSFER TO ANOTHER PERSON

If you wish someone else to see this document, send in name with document and the library will arrange a loan.

OAK RIDGE NATIONAL LABORATORY
OPERATED BY
CARBIDE AND CARBON CHEMICALS DIVISION
UNION CARBIDE AND CARBON CORPORATION
UCC
POST OFFICE BOX P
OAK RIDGE, TENNESSEE

UNCLASSIFIED

U N C L A S S I F I E D

Report Number: ORNL-933

This document consists of 44 pages.
Copy 8 of 217 Series B

Contract No. W-7405, eng-26

Physics Division

TRANSPORT PARAMETERS FOR THERMAL NEUTRONS IN WATER

by

Francis Joseph Sisk*
Lieutenant, United States Navy

Date Issued: MAR 15 1951

OAK RIDGE NATIONAL LABORATORY
Operated By
CARBIDE AND CARBON CHEMICALS DIVISION
Union Carbide and Carbon Corporation
Post Office Box P
Oak Ridge, Tennessee

*Submitted in partial fulfillment of the requirements for the degree of Master of Science.

MARTIN MARIETTA ENERGY SYSTEMS LIBRARIES

U N C L A S S I F I E D

3 4456 0352739 7

INTERNAL DISTRIBUTION

1. G. T. Felbeck (C&CCD)
2-3. Chemistry Library
4. Physics Library
5. Biology Library
6. Health Physics Library
7. Metallurgy Library
8-9. Training School Library
10-13. Central Files
14. C. E. Center
15. C. E. Larson
16. W. B. Humes (K-25)
17. W. D. Lavers (Y-12)
18. A. M. Weinberg
19. J. A. Swartout
20. E. D. Shipley
21. E. J. Murphy
22. F. C. VonderLage
23. A. H. Snell
24. E. H. Taylor
25. A. Hollaender
26. K. Z. Morgan
27. F. L. Steahly
28. M. T. Kelley
29. W. H. Pennington
30. E. O. Wollan
31. D. W. Cardwell
32. A. S. Householder
33. L. D. Roberts
34. J. A. Lane
35. M. M. Mann
36. R. N. Lyon
37. W. C. Koehler
38. W. K. Ergen
39. E. P. Blizard
40. F. J. Sisk
41. M. J. Skinner
42. E. C. Campbell
43. C. C. Harris
44. R. J. Stephenson
45. E. D. Klema
46. H. S. Pomerance
47. W. S. Snyder
48. D. K. Holmes
49. G. B. Arfkin, Jr.
50-51. Central Files (O.P.)

EXTERNAL DISTRIBUTION

52-63. Argonne National Laboratory
64. Armed Forces Special Weapons Project
65-70. Atomic Energy Commission, Washington
71. Battelle Memorial Institute
72. Brush Beryllium Company
73-76. Brookhaven National Laboratory
77. Bureau of Medicine and Surgery
78. Bureau of Ships
79-82. Carbide and Carbon Chemicals Division (K-25 Plant)
83. Columbia University (J. R. Dunning)
84. Columbia University (G. Failla)
85-89. E. I. du Pont de Nemours and Company
90-93. General Electric, Richland
94-97. Idaho Operations Office
98-99. Iowa State College
100. Kansas City Operations Branch
101. Kellex Corporation
102-103. Kirtland Air Force Base
104-107. Knolls Atomic Power Laboratory
108-110. Los Alamos Scientific Laboratory
111. Mallinckrodt Chemical Works
112. Massachusetts Institute of Technology (A. Gaudin)
113. Massachusetts Institute of Technology (A. R. Kaufmann)
114-116. Mound Laboratory
117. National Advisory Committee for Aeronautics
118. National Bureau of Standards (R. D. Huntoon)
119. Naval Medical Research Institute
120-121. Naval Radiological Defense Laboratory
122. New Brunswick Laboratory
123-125. New York Operations Office
126. North American Aviation, Inc.

127-130. Carbide and Carbon Chemicals Division (Y-12)
131. Patent Branch, Washington
132. RAND Corporation
133. Sandia Corporation
134. Santa Fe Operations Office
135-149. Technical Information Service, Oak Ridge
150-152. USAF, NEPA Office
153-154. U. S. Geological Survey (T. B. Nolan)
155-156. U. S. Public Health Service
157. University of California at Los Angeles
158-162. University of California Radiation Laboratory
163-164. University of Rochester
165. University of Washington
166. U. S. Atomic Energy Commission (Wilmington)
167. Western Reserve University
168-171. Westinghouse Electric Corporation
172. Yale University
173-176. Atomic Energy Project, Chalk River
177. Chief of Naval Research
178. H. K. Ferguson Company
179. Harshaw Chemical Company
180. Isotopes Division (Mr. McCormick)
181-182. Library of Congress, Acquisition Department (J. W. Cormn)
183. National Bureau of Standards
184. National Research Council, Ottawa
185. Naval Research Laboratory
186-187. Nevis Cyclotron Laboratories
188. Nucleonics
189-190. Oak Ridge Institute of Nuclear Studies
191-200. United Kingdom Scientific Mission (M. Greenhill)
201. USAF, Eglin Air Force Base (Technical Library)
202. USAF, Wright-Patterson Air Force Base (Rodney Nudenberg)
203-207. USAF, Wright-Patterson Air Force Base (CADO)
208. U. S. Army, Army Field Forces (Captain James Kerr)
209. U. S. Army, Atomic Energy Branch (Lt. Col. A. W. Betts)
210. U. S. Army, Director of Operations Research (Dr. Ellis Johnson)
211. U. S. Army, Office, Chief of Ordnance (Col. A. R. Del Campo)
212-213. U. S. Army, Office of the Chief Signal Officer (Curtis T. Clayton thru Major George C. Hunt)
214-216. U. S. Army, Technical Command (Col. J. H. Rothschild Attn: Technical Library)
217. UT-AEC Agricultural Research Program (Charles S. Hobbs)

PREFACE

This problem was first considered in April, 1950, and experimental work was performed in August and September 1950, employing the laboratory facilities of the Oak Ridge School of Reactor Technology at Oak Ridge National Laboratory, Oak Ridge, Tennessee. At first it was desired simply to demonstrate that the theory of neutron transport yields adequate predictions for the neutron flux in normal water near boundaries. It soon became clear that appropriate average values of the neutron cross sections for normal water (required to solve the transport problem) are not accurately known. It was then proposed to determine those "appropriate average values" which best fit the transport solutions to experiment. These numbers are, of course, useful in the design of water-moderated reactors and in other applications of neutron physics.

Grateful acknowledgment is due Dr. E. C. Campbell of Oak Ridge National Laboratory who was a constant source of invaluable advice.

TABLE OF CONTENTS

		Page
Chapter I.	Introduction and Summary	1
	1. Introduction	1
	2. Summary	4
Chapter II.	Transport Theory and Methods of Analysis	5
Chapter III.	Experimental Procedure	22
Bibliography		32
Appendix I		33
Appendix II		37

LIST OF ILLUSTRATIONS

		Page
1.	Velocity Diagram for Two-Body Collision	26
2.	Integration for Plane Kernel - Transport Equations	27
3.	Foil Mount and Cadmium Plane Assembly	28
4.	Thermal Neutron Flux in Water Near a Black Plane	29
5.	One-Dimensional Thermal Neutron Flux in Water Near a Black Boundary	30
6.	Diametral Flux Distribution	31

CHAPTER I

INTRODUCTION AND SUMMARY

1. Introduction

The steady state spatial distribution of neutron fluxes in matter is a problem of prime importance to the designer of chain reacting piles, and has been the subject of very much theoretical and experimental work. The case in which the neutron energy is large compared to that of the nuclei constituting the medium (the "slowing down" case) is of first importance and is rather extensively investigated. The alternate case in which the neutrons are in energy equilibrium with the medium is of lesser importance and comparatively little experimental work has been done, although the fundamental theory is well in hand. The cross-sections for neutron scattering and absorption appropriate to the first case are the "ordinary" energy-dependent cross-sections (or simple functions of these) which have been so extensively investigated by various neutron spectrometry groups. The cross-sections appropriate to the second case are more vaguely defined. Perhaps as adequate a definition of these parameters as any is the "ad hoc" one - those numbers which, when inserted in the mathematical theory of particle transport yield proper solutions for the neutron flux. It can be demonstrated that these numbers are not in general the average values of the energy dependent cross sections weighted by the appropriate energy distribution function for the ambient temperature.

The "ad hoc" definition suggests a means of experimentally measuring the numbers. One requires a medium - of simple geometry so that the transport problem is soluble - in which a flux of thermal equilibrium neutrons

is maintained and in which the flux can be measured at various points with neutron detectors. Since two parameters are to be determined, two independent solutions for the flux must be available - but this is easily provided for by considering (1) a region "remote" from discontinuities in which the solution is asymptotic and (2) a region adjacent to a discontinuity - say a "black" boundary. One measures the flux at a sufficient number of points in each region to define the spatial functions. The transport problem is solved many times for various values of the parameters, and if fortune is good one pair of values will be found to yield solutions which fit the experimental functions in both regions.

To particularize - the chosen medium is normal water, the geometry one-dimensional consisting of a tank many mean free paths in its dimensions, traversed by a uniform thermal neutron current arriving at one face and absorbed by a layer of cadmium at the opposite face. The neutron flux is measured at points along a line normal to the cadmium facing and extending from the facing well into region (1).

The one-dimensional transport problem is integrable in closed form for region (1). This solution is matched to the experimental data, yielding a characteristic equation in say the total cross-section and the scattering cross-section - thus the scattering section may be eliminated. The transport problem is then integrated numerically in region (2) for various values of total cross section and that value selected which yields best fit with experimental data. Unfortunately, this straight-forward procedure could not be carried out. It was found that numerical integration produced a function which fit the experimental data astonishingly well, but that the values of the parameter which yielded this good fit were variable with

respect to the integrating procedure. Further, it was found that each improvement in the integrating plan led monotonously to a reduction in the total cross section, indicating that the process of improving the operation was not near convergence. The rapid increase in computing labor made it necessary to abandon this process before a firm solution was obtained.

The Wiener-Hopf method, treated by Frankel and Goldberg (3), offers a general solution to the one-dimensional transport problem in a single semi-infinite medium. However, it is available only as an exceedingly difficult double numerical quadrature which could not be handled for lack of computing facility. A solution is given for the flux at the black boundary only, requiring only one numerical quadrature. By equating this solution in terms of the parameters to the experimental value of the "contact" flux, unique values are obtained for the parameters. These values extrapolate the trend of the numerical solutions, and are in that sense to be regarded as supported by the numerical method.

The convergence on the Wiener-Hopf solution may be illustrated by the successive values for the macroscopic "total" cross section. They are: Numerical - 2.9 cm^{-1}; 2.5 cm^{-1} and 2.3 cm^{-1}; Wiener-Hopf - 2.10 cm^{-1}.

2. Summary

Findings may be tabulated as follows:

Parameter - Water at 24° C.	Values
Diffusion Length	2.67 ± .02 cm.
Transport Mean Free Path	0.48 ± .01 cm.
Absorption Mean Path (Equivalent)	44.2 ± 1.3 cm.
Microscopic Transport Cross Section	62.4 ± 1.5 barns/mol.
Microscopic Absorption Cross Section (Equivalent)	0.68 ± 0.01 barns/mol.
Ratio - Boundary Flux ÷ Asymptotic (Exponential) Flux	0.186
Ratio - Boundary Flux ÷ Asymptotic (Hyperbolic) Flux	0.87
Extrapolation Distance - X_0	0.32 cm.
Ratio - Extrapolation Distance/Total Mean Path	0.67

Comparison of the cross-section with the energy-dependent values for protons in water by Bacher(1) and Melkonian (7) indicate an "average" neutron energy for transport of perhaps 0.05 electron volts in contrast with the Maxwell-Boltzmann mode of 0.025 e.v. This is not surprising since it is expected that transport is largely effected by the high energy neutrons which have longer free paths. In addition it must be remembered that the neutron flux is weighted by a velocity term so that the average flux corresponds to a higher energy than does the average neutron, and transport weights the cross-section by the flux rather than by the neutron density. The $1/v$ absorption in hydrogen provides a preferential sink for low energy neutrons, thus the thermal distribution is displaced from the Maxwell-Boltzmann toward higher energy.

CHAPTER II

TRANSPORT THEORY AND METHODS OF ANALYSIS

To indicate the assumptions involved and to portray the physical model which was analyzed, it may be well to review the fundamental theory of neutron transport. It must be emphasized that the model of neutron transport for neutrons in energy equilibrium with the medium, at energies well below the atomic binding, differs radically from that for energetic neutrons ($E_n > 1$ ev) in media at normal temperature.

In the latter case the energy transfer in neutron-nucleus interactions is uniformly from neutron to nucleus, the nuclei interact as free particles, and since the atomic vibrational energy is comparatively small, the nuclei may be regarded as initially at rest. None of these statements hold for the former case.

In the present problem, by definition, the net average energy transfer between neutrons and medium is very small and due solely to the preferential absorption of the slower neutrons. The protons are bound in the molecule with energy larger than the neutron energy and the nuclei cannot interact as free particles. The thermal motion of the atoms and of the systems in which they are bound is not negligible, and so affects not only the mechanics of the collisions but also the frequency of occurrence since the collision probability is a function of the flux of nuclei as well as of neutrons.

Inelastic interaction of neutrons with rotational and vibrational levels of the water molecule are probably present. The rotational levels are quite numerous and begin at wave number 23.8 cm^{-1}, (about .003 electron volts) according to Wu (9).

Quantitive discussion of the scattering mechanism in a system as

complex as this is not in the scope of this paper. However to avoid misinterpretation of the results, it is necessary to consider at least the question of whether the scattering is symmetric, that is whether all values of the angle of deflection of the neutron in the Laboratory System are equally probable, when the neutrons are in energy equilibrium with the medium.

Referring to Fig. (1), $\bar{v}_0$ and $\bar{v}$ are the velocities of neutron and molecule respectively before collision, in the laboratory system, and ω the angle between them. To transfer to the center of mass system a vector velocity $\bar{V}$ is added of such magnitude and direction as to reduce the total momentum to zero. Using unity as neutron mass and M as molecule mass we have:

$$v_0 + V_x + M(v \cos \omega + V_x) = 0$$

and

$$V_y + M(v \sin \omega + V_y) = 0$$

thus

$$V_x = -\frac{M}{M+1} v \cos \omega - \frac{1}{M+1} v_0$$

and

$$V_y = -\frac{M}{M+1} v \sin \omega$$

where V_x and V_y are the scalar components of $\bar{V}$.

The transformation vector is thus seen to resolve into two vectors, one of magnitude $\frac{M}{M+1} v$ and opposite to $\bar{v}$ in direction, and one of magnitude $\frac{1}{M+1} v_0$ and opposite to $\bar{v}_0$ in direction. The vectors $\bar{v}_0'$ and $\bar{v}'$ are the velocities before collision in C.M. system and $\bar{v}_0''$ and $\bar{v}''$ are the C.M. velocities after collision. If the scattering is spherically symmetric in C. M. system, all values of $\cos \psi$, the deflection angle, are equally probable. To obtain the neutron velocity u, after collision, in

Laboratory system, we add $(-\bar{V})$ vectorially to $\bar{v}_0''$. The probability of ω is $\sin\omega$, and is therefore symmetric, so on the average the contribution of $\frac{M}{M+1}\bar{v}$ involves no preferred direction. However, the contribution of $\frac{1}{M+1}\bar{v}_0$ inserts the direction of the incoming neutron as a component of u. Thus the scattered neutrons will emerge from collisions preferentially in the direction of their pre-collision motion with a weight increasing with neutron energy.

The preferentially forward scattering, as indicated, correlates rather poorly the direction of each path with the preceding one, less well with the next but one preceding, and after a large number of intervening scatterings the correlation vanishes. One may attempt to obtain the number of neutrons passing through a small volume increment ($d\mathcal{V}$) by summing up those neutrons scattered in all other volume increments ($d\mathcal{V}'$) in the space which reach the first increment in free flight. However, since the number of scattered neutrons leaving $d\mathcal{V}'$ in the direction of $d\mathcal{V}$ depends on the average direction of the neutrons entering $d\mathcal{V}'$, this average direction must be found by another summing up of previously scattered neutrons and so on. The mathematical analysis of such a situation yields infinite order multiple integrals, so simplification is necessary. The difficulty does not occur if the scattering is isotropic, so an obvious suggestion might be to approximate the system with a model in which the scattering is isotropic.

If one considers a neutron scattered isotropically at a point in a non-absorbing medium and asks for the probability of finding it at any point in the space after the lapse of a long time, it is clear that the resulting probability field is symmetric about the initial point. Analogously, one considers a neutron with initial motion $\bar{v}_0$ scattered at a point anisotropically in the Lab system but isotropically in C.M. system.

The probability of finding the once scattered neutron at position $\bar{r}$ is then symmetric about the moving center of mass whose velocity is $\frac{1}{M+1}\bar{v}_0$. However, the probability of finding the second scattered neutron at $\bar{r}$ is only azimuthally symmetric since each spherical shell of second scattered neutron probability is immediately again retarded by the factor $\frac{1}{M+1}$, corresponding to the motion of the center of mass of the second scattering system. Thus the second scattered neutrons which have made long flight after first scattering will be found on the average farther along in the direction of $\bar{v}_0$ than those which make short flights. In spite of the forbidding complexity of the picture some information can be obtained about the probability distribution after a large number of collisions. The path lengths ℓ, the azimuthal scattering angles ϑ, and the cosines of the polar scattering angles μ, are every one statistically independent, and may be averaged independently. The centroid of the distribution is obviously found in the direction of $\bar{v}_0$ and may be located by first averaging over the azimuthal angles starting with the last flight. One obtains $(\ell_1\mu_1 + \ell_2\mu_2\mu_1 + \ldots \ell_n \prod_1^n \mu_n + \ldots)$. Averaging over ℓ_n and μ_n one has

$$\bar{\ell} = \iint \mu_1 P(\mu_1)\ell_1 P(\ell_1)\, d\mu_1\, d\ell_1 + \iiint \mu_1 P(\mu_1)\mu_2 P(\mu_2)\ell_2 P(\ell_2)\, d\mu_1\, d\mu_2\, d\ell_2 + \ldots$$

The required first moment is then $\lambda_s(\bar{\mu} + \bar{\mu}^2 + \bar{\mu}^3 + \ldots \bar{\mu}^n + \ldots)$ which is the expansion of $\frac{\lambda_s\bar{\mu}}{1-\bar{\mu}}$. One concludes then that the average position, after very many scatterings, of a neutron projected from a point in a medium is at a distance $\lambda_s(1 + \frac{\bar{\mu}}{1-\bar{\mu}})$ or $\frac{\lambda_s}{1-\bar{\mu}}$ from the initial point. This parameter is called the transport mean free path. The higher moments of the probability function are not available in general.

F. Joliot (5) has computed the probability function itself for the nth isotropic scattering in a quite complicated series of Hermite polynomials.

One may now reasonably postulate that the scattering mechanism in an anistropically scattering medium may be rather well reproduced by an isotropic model, provided that the scattering length be weighted by the factor $\frac{1}{1 - \bar{\mu}}$. This ignores the defect that the higher moments are not properly scaled.

It must be emphasized that capture has not been considered and that the model is not correct for large capture. It then remains to be demonstrated that the model is satisfactory if capture is small but not negligible.

The simplified transport model now may be more clearly defined. It consists of a three dimensional array of fixed lattice points at which the neutrons scatter isotropically, or are absorbed.

The scattering length in the model is the transport free path in the real medium and is in general not known. The absorption free path in the model is not in general the same as the absorption length in the medium but is probably nearly the same if absorption is small. A more useful pair of parameters are the inverses of the free paths - the macroscopic cross sections - defined as the probability per centimeter of path of the defined event. To prove the relation:

$$-dI = I \Sigma \, d\ell$$

Where I is the beam intensity

$$I = I_0 \epsilon^{-\Sigma \ell}$$

Let $I_0 = 1$, $I = \epsilon^{-\Sigma \ell}$

The mean value of ℓ is:

$$\lambda = \frac{\int_0^\infty \ell \epsilon^{-\Sigma \ell} d\ell}{\int_0^\infty \epsilon^{-\Sigma \ell} d\ell} = \frac{1}{\Sigma}$$

A macroscopic absorption cross-section is similarly defined.

The following notation is to be used:

n - Neutron density, cm^{-3}

φ - Neutron scalar flux density, called simply "flux," cm^{-2} sec^{-1}

Σ_t - Mean macroscopic transport cross section, cm^{-1}

Σ_a - Mean macroscopic absorption cross section cm^{-1}

Σ - Mean total cross section, cm^{-1}

N - Lattice point density of the medium, cm^{-3}

σ - Microscopic total cross section, cm^2

x - Distance, cm.

z - Distance in mean paths

$\bar{r}$ - Position vector

One asks for the number of neutrons scattered in incremental volume at position $\bar{r}$ and crossing unit normal area at $\bar{r}'$ per second. The total scattered at $\bar{r}$ is $\varphi(\bar{r})\Sigma_t d\mathcal{V}$ - all cross sections being independent of $\bar{r}$ in the homogeneous medium - and of these $\frac{1}{4\pi} d\omega$ leave $\bar{r}$ in $d\omega$ about solid angle ω. Since the area subtended at $\bar{r}'$ by $d\omega$ at $\bar{r}$ is $(\bar{r}' - \bar{r})^2 d\omega$, a division by this factor is indicated, and since the beam in any $d\omega$ is attenuated by absorption and re-scattering as $\epsilon^{-\Sigma_t|\bar{r}'-\bar{r}|}\,\epsilon^{-\Sigma_a|\bar{r}'-\bar{r}|}$, multiplication by this last factor is required. The required number is then $\dfrac{\varphi(\bar{r})\Sigma_t\,\epsilon^{-\Sigma|\bar{r}'-\bar{r}|}\,d\mathcal{V}}{4\pi(\bar{r}'-\bar{r})^2}$

The neutron flux at $\bar{r}'$ is then obtained by summing up the neutrons scattered at all $\bar{r}$ and crossing unit area at $\bar{r}'$. Thus

$$\varphi(\bar{r}') = \frac{1}{4\pi}\Sigma_t \int_{SPACE} \frac{\varphi(\bar{r})\,\epsilon^{-\Sigma|\bar{r}'-\bar{r}|}}{(\bar{r}'-\bar{r})^2}\, d\mathcal{V}$$

In the problem at hand, the medium is considered to be a semi-infinite slab - infinite in horizontal extent and downward, its upper face bounded by a plane from which no neutrons return, and having a finite neutron current passing upward through it. The coordinate x is measured from the "black" plane and normal to it. In this system the flux is a function of x alone.

One requires the number of neutrons scattered in an incremental slab dx at x and passing in free flight through unit area about a point at x'. Referring to Fig. 2, this quantity called $K_{(|x'-x|)}dx$ is found as follows:

$$K\,dx = \frac{\varphi(x)\Sigma_t}{4\pi}\int_{r=0}^{\infty}\frac{e^{-\Sigma\rho}}{\rho^2}\,(2\pi r\,dr\,dx)$$

$$r^2 + (x'-x)^2 = \rho^2$$

$$r\,dr = \rho\,d\rho$$

$$K = \frac{\varphi(x)\Sigma_t}{2}\int_{\rho=|x'-x|}^{\infty}\frac{e^{-\Sigma\rho}}{\rho}\,d\rho$$

$$K = \frac{\varphi(x)\Sigma_t}{2}\int_{\Sigma|x'-x|}^{\infty}\frac{e^{-\Sigma\rho}}{\Sigma\rho}\,d(\Sigma\rho)$$

The integral is termed $E_1(\Sigma|x'-x|)$, the exponential integral, and is identical with the function $-E_i(-x)$ as tabulated by Jahnke & Ehmde and others.

The flux at x' is obtained by summing the contributions of all increments dx at x as follows:

$$\varphi(x') = \frac{\Sigma_t}{2}\int_{space} \varphi(x)\, E_1(\Sigma|x'-x|)\, dx$$

This linear integral equation is perhaps more conveniently handled in mean free path dimensions as follows:

$$\varphi(z') = \frac{\Sigma_t}{2\Sigma}\int \varphi(z)\, E_1(|z'-z|)\, dz$$

For the configuration space described, the limits of integration are zero and plus infinity. However as $z \geq \sim 15$ the contribution to the integral between negative infinity and zero becomes negligibly small, and the limits may be taken, with vanishing error, over all values of z. In this asymptotic form the equation has a simple hyperbolic solution.

The usual method of treatment, to indicate the form of the asymptotic solution (as in Frankel & Nelson (4)), involves transforming the origin to write:

$$\varphi(z') = \frac{\Sigma_t}{2\Sigma}\int_{-\infty}^{\infty} \varphi(z'+z)\, E_1(z)\, dz$$

and expand $\varphi(z'+z)$ in Taylor's series about z':

$$\varphi(z') = \frac{\Sigma_t}{2\Sigma}\int_{-\infty}^{\infty} E_1(|z|)\left[\varphi(z') + z\varphi'(z') + \frac{z^2}{2!}\varphi''(z') + \cdots\right] dz$$

Now $\mathfrak{M}_m = \int_{-\infty}^{\infty} z^m E_1(|z|)\, dz$ is the mth moment of the kernel

about its origin, and this vanishes by symmetry for m odd. One has then

$$\varphi_{(z')} = \frac{\Sigma_t}{2\Sigma}\left[m_0 \varphi_{(z')} + \frac{m_2}{2} \varphi''_{(z')}\right]$$

neglecting terms above the third order. Rearranging, one has the one-dimensional differential equation of elementary diffusion theory - the Helmholtz equation:

$$\varphi'' + \left(\frac{2m_0}{m_2} - \frac{4\Sigma}{m_2\Sigma_t}\right)\varphi = 0$$

for which the solutions are hyperbolic if $m_0 < \frac{2\Sigma}{\Sigma_t}$, circular if $m_0 > \frac{2\Sigma}{\Sigma_t}$, and linear if $m_0 = \frac{2\Sigma}{\Sigma_t}$. Now $m_0 = \int_{-\infty}^{\infty} E_{1(|z|)} dz = 2$, and if absorption is present, then $\Sigma > \Sigma_t$, so $m_0 = 2 < \frac{2\Sigma}{\Sigma_t}$. Thus we expect hyperbolic solutions, so a trial function $\varphi_{(z)} = \epsilon^{-\kappa z}$ is substituted in the integral equation, and the integration performed at the point $z' = 0$

$$1 = \frac{\Sigma_t}{2\Sigma}\int_{-\infty}^{\infty} \epsilon^{-\kappa z} E_{1(|z'-z|)}\, dz$$

$$= \frac{\Sigma_t}{2\Sigma}\left\{\int_{-\infty}^{0} \epsilon^{-\kappa z} E_{1(-z)}\, dz + \int_{0}^{\infty} \epsilon^{-\kappa z} E_{1(z)}\, dz\right\}$$

$$= \frac{\Sigma_t}{2\Sigma}\left\{\int_{0}^{\infty} \epsilon^{+\kappa z} E_{1(z)}\, dz + \int_{0}^{\infty} \epsilon^{-\kappa z} E_{1(z)}\, dz\right\}$$

$$= \frac{\Sigma_t}{\Sigma}\int_{0}^{\infty} \cosh(\kappa z) E_{1(z)}\, dz$$ which is integrated by parts after putting $E_{1(z)}$ in integral form.

$$1 = \frac{\Sigma_t}{\Sigma}\int_{0}^{\infty} \cosh(\kappa z)\, dz \int_{z}^{\infty} \frac{\epsilon^{-y}}{y}\, dy$$

$$1 = \frac{\Sigma_t}{\Sigma}\left[\frac{1}{\mathcal{R}}\sinh(\mathcal{R}z)\,E_1(z)\right]_0^\infty + \frac{\Sigma_t}{\mathcal{R}\Sigma}\int_0^\infty \sinh(\mathcal{R}z)\,\frac{e^{-z}}{z}\,dz$$

The first integral vanishes for $\mathcal{R}<1$ since at upper limit $E_1(z)$ is of order e^{-z} and at lower limit $\frac{\sinh \mathcal{R}z}{\mathcal{R}}$ goes as z and the singularity of $E_1(z)$ is logarithmic. Writing the second integral in exponential form

$$1 = \frac{\Sigma_t}{2\mathcal{R}\Sigma}\int_0^\infty \frac{e^{-z(1-\mathcal{R})} - e^{-z(1+\mathcal{R})}}{z}\,dz$$

and separating the range of integration into intervals:

$$1 = \frac{\Sigma_t}{2\mathcal{R}\Sigma}\left\{\int_0^{1/1-\mathcal{R}} \frac{e^{-z(1-\mathcal{R})}}{z}dz - \int_0^{1/1+\mathcal{R}} \frac{e^{-z(1+\mathcal{R})}}{z}dz + \int_{\frac{1}{1-\mathcal{R}}}^{\infty} \frac{e^{-z(1-\mathcal{R})}}{z}dz - \int_{\frac{1}{1+\mathcal{R}}}^{\infty} \frac{e^{-z(1+\mathcal{R})}}{z}dz\right\}.$$

the third and fourth integrals are seen to be each $E_1(1)$ and cancel, thus

$$1 = \frac{\Sigma_t}{2\mathcal{R}\Sigma}\ln\frac{1+\mathcal{R}}{1-\mathcal{R}}$$

or $$\frac{\Sigma_t}{\Sigma} = \frac{\mathcal{R}}{\frac{1}{2}\ln\frac{1+\mathcal{R}}{1-\mathcal{R}}} = \frac{\mathcal{R}}{\tanh^{-1}\mathcal{R}}$$

expanding in power series

$$\frac{\Sigma}{\Sigma_t} = 1 + \frac{\mathcal{R}^2}{3} + \frac{\mathcal{R}^4}{5} + \ldots + \frac{\mathcal{R}^{2n}}{2n+1}$$

Inverting the series in $\mathcal{R}^2$ we obtain

$$\mathcal{R}^2 = 3\frac{\Sigma_a}{\Sigma_t} - \frac{9}{5}\left(\frac{\Sigma_a}{\Sigma_t}\right)^2 - 1.851\left(\frac{\Sigma_a}{\Sigma_t}\right)^3 + \ldots$$

Note that $e^{-\mathcal{R}z}$ is an eigen function in mean free path measure and the function in cm. measure is e^{-kx} where $k = \mathcal{R}\Sigma$.

Given an experimental value of k (which is simply the logarithmic slope of the flux distribution plotted against x) one may choose a value of Σ , compute κ by $\kappa = k/\Sigma$, and using the series in κ^2 (or any conveniently obtained solution) compute Σ_t/Σ . Returning to the integral equation

$$\varphi(z) = \frac{\Sigma_t}{2\Sigma}\int_0^\infty \varphi(z')\, E_1(|z'-z|)\, dz'$$

one may insert the computed value of Σ_t/Σ . It is now required to compute the eigenfunction $\varphi(z)$ corresponding to the selected value of Σ . A choice of method is available.

LeCaine (6) has treated the problem by a variational method, presenting tabulated values for the flux normalized to unit flux at the black plane for various values of Σ_a/Σ_t . A rather rough solution for the parameters is available by using these results, and indicates that Σ lies between 2.0 cm^{-1} and 2.4 cm^{-1}.

It was then decided to attempt solution by a direct numerical method, which was carried out to completion. In theory the method goes as follows: Given the integral equation as before

$$\varphi(z) = \frac{\Sigma_t}{2\Sigma}\int_0^\infty \varphi(z')\, E_1(|z'-z|)\, dz'$$

The integral is replaced by a Riemann sum equation

$$\varphi(z_i) = \frac{\Sigma_t}{2\Sigma}\Delta z \sum_n \varphi(z_n)\, E_1(|z_i - z_n|)$$

which may be put in matrix notation

$$\begin{bmatrix} Z_0 \\ Z_1 \\ \vdots \\ Z_i \end{bmatrix} = \frac{\Sigma_t}{2\Sigma} \Delta Z \begin{bmatrix} E_{00} & E_{01} & E_{02} & - & - & - & E_{0n} \\ E_{10} & E_{11} & E_{12} & - & - & - & - \\ E_{20} & E_{21} & E_{22} & - & - & - & - \\ - & - & - & - & - & - & - \\ - & - & - & - & - & - & - \\ E_{i0} & - & - & - & - & - & E_{in} \end{bmatrix} \begin{bmatrix} Z_0 \\ Z_1 \\ Z_2 \\ - \\ - \\ Z_n \end{bmatrix}$$

where E_{in} is the absolute value of the exponential integral of argument $(i-n)\Delta Z$. At the argument i = n the exponential integral is singular, so a mean value was computed for this range. One requires:

$$\frac{2}{\Delta Z}\int_0^{\frac{\Delta Z}{2}} E_1(Z)\,dZ = \frac{2}{\Delta Z}\int_0^{\frac{\Delta Z}{2}} dZ \int_1^{\infty} \frac{e^{-yZ}}{y}\,dy$$

$$= \frac{2}{\Delta Z}\int_1^{\infty} \frac{dy}{y}\int_0^{\frac{\Delta Z}{2}} e^{-yZ}\,dZ = \frac{2}{\Delta Z}\int_1^{\infty}\left(\frac{1}{y^2} - \frac{e^{-y\Delta Z}}{y^2}\right)dy$$

$$= \frac{2}{\Delta Z}\left(1 - e^{-\frac{\Delta Z}{2}}\right) + E_1\left(\frac{\Delta Z}{2}\right)$$

The integrating scheme is the equivalent of the trapezoidal rule but employing the function of mean argument instead of the chordal mean as the summation element.

One proceeds by inserting a tabular trial function, performing the matrix operation as indicated and emerging with a new and bettered function which is iterated until the variation produced by iteration is insignificant.

In practice minor departures from the straight forward process were introduced to reduce the labor. The principal one of these consisted in iterating for only about 10 terms of the flux vector and writing the complete vector by smoothing the first differences.

A variant of this scheme was considered, which involved writing the equation in a perturbation form:

$$\varphi_a(z) - \delta(z) = \frac{\Sigma_t}{2\Sigma}\int_{-\infty}^{\infty}\left[E_1(|z'-z|) - \varepsilon(|z'-z|)\right]\left[\varphi_a(z) - \delta(z)\right]dz$$

where φ_a is the asymptotic solution, δ is the boundary depression, and ε is the perturbation of the operator E_1 required to extend the integration over all z .

$$\delta(z) = \frac{\Sigma_t}{2\Sigma}\int_{-\infty}^{\infty}\left\{\left[E_1(|z'-z|) - \varepsilon(|z'-z|)\right]\delta(z) + \varepsilon\varphi_a\right\}dz$$

or in Riemann sum form

$$\delta_i = \frac{\Sigma_t}{2\Sigma}\Delta z\sum_n\left[E_1-\varepsilon\right]_{(|z_i-z_n|)}\delta_n + \sum_n \varepsilon_{(|z_i-z_n|)}\varphi_a$$

The equivalent matrices, all infinite order are:

$$\varphi_a = \begin{bmatrix} - \\ - \\ - \\ \varphi_{-2} \\ \varphi_{-1} \\ \varphi_1 \\ \varphi_2 \\ - \\ - \\ - \end{bmatrix} \qquad \delta = \begin{bmatrix} - \\ - \\ - \\ \varphi_{-2} \\ \varphi_{-1} \\ \delta_1 \\ \delta_2 \\ - \\ - \\ - \end{bmatrix} \qquad \varepsilon = \begin{bmatrix} - & - & - & - & - & - \\ - & - & - & - & - & - \\ - & E_{-2-2} & E_{-2-1} & E_{-21} & E_{-22} & - \\ - & E_{-1-2} & E_{-1-1} & E_{-11} & E_{-12} & - \\ - & E_{1-2} & E_{1-1} & 0 & 0 & 0 \\ - & E_{2-2} & E_{2-1} & 0 & 0 & 0 \\ - & - & - & 0 & 0 & 0 \end{bmatrix}$$

$$E - \mathcal{E} = \begin{bmatrix} 0 & 0 & 0 & 0 & 0 & 0 & 0 & 0 \\ 0 & 0 & 0 & 0 & 0 & 0 & 0 & 0 \\ 0 & 0 & 0 & 0 & 0 & 0 & 0 & 0 \\ 0 & 0 & 0 & 0 & 0 & 0 & 0 & 0 \\ 0 & 0 & 0 & E_{11} & E_{12} & E_{13} & - & - \\ 0 & 0 & 0 & E_{21} & E_{22} & E_{23} & - & - \\ 0 & 0 & 0 & E_{31} & E_{32} & E_{33} & - & - \\ 0 & 0 & 0 & - & - & - & - & - \\ 0 & 0 & 0 & - & - & - & - & - \end{bmatrix}$$

The first method has the disadvantage that the term products converge rather slowly for increasing z so that each term of the iterated vector represents very many term products and the computation is quite laborious. The second method avoids this trouble since δ vanishes strongly with increasing z, but δ varies so rapidly near $(z = 0)$ that trapezoidal integration is valid only for a very small interval Δz. On balance, method one appeared most feasible and was chosen. A value of 2.9 cm^{-1} was obtained for Σ with a very fine fit of the solution to the experimental data.

To investigate the validity of the integration, the process was then repeated with an improved kernel. In this case the matrix elements were obtained by computing mean values for the exponential integral with a unit weight function for each Δz_n. This process amounts to correcting for variation of the kernel over the interval but ignoring the variation of the function. A value of $\Sigma = 2.5$ cm^{-1} resulted.

A further improvement in the kernel was then tried. One assumes that the function may be linearized with small error over the interval Δz.

The matrix equation is then written:

$$\varphi_{(z_i)} = \frac{\Sigma_t}{2\Sigma} \sum_n \int_0^{\Delta z} \left[\varphi_{(z_n)} + \frac{\Delta\varphi_n}{\Delta z} \zeta \right] E_{1(|z_i - z_n + \zeta|)} \, d\zeta$$

where z_n is the lower boundary of the nth interval, Δz is the width of the interval, $\Delta\varphi_n$ is the difference $\left[\varphi_{(z_{n+1})} - \varphi_{(z_n)} \right]$, and ζ is the difference $\left[z - z_n \right]$. The equation may be separated into two terms as follows:

$$\varphi_{(z_i)} = \frac{\Sigma_t}{2\Sigma} \sum_n \left[\varphi_{(z_n)} \int_0^{\Delta z} E_{1(|z_i - z_n + \zeta|)} \, d\zeta + \frac{\Delta\varphi_n}{\Delta z} \int_0^{\Delta z} \zeta E_{1(|z_i - z_n + \zeta|)} \, d\zeta \right]$$

The first integral (letting $y = |z_i - z_n + \zeta| = |K_n + \zeta|$)

$$I_{1,n} = \int_{K_n}^{K_{n+1}} E_{1(y)} \, dy = e^{-K_n} - e^{-K_{n+1}} - K_n E_{1(K_n)} + K_{n+1} E_{1(K_{n+1})}$$

The second integral, dropping absolute values:

$$I_{2,n} = \int_{K_n}^{K_{n+1}} (y - K_n) E_{1(y)} \, dy$$

$$= \frac{1}{2} \left[e^{-K_n}(1 + K_n) - e^{-K_{n+1}}(1 + K_{n+1}) + K_{n+1}^2 E_{1(K_{n+1})} - K_n^2 E_{1(K_n)} \right] - K_n I_{1,n}$$

I_1 constitutes the terms of an operator which operates on the function φ_n and I_2 an operator which operates on the relative increment of the function, $\Delta\varphi_n / \Delta z$.

The process yielded again an excellent fit to the data but for a value $\Sigma = 2.3\ \mathrm{cm}^{-1}$. Since the computing had become impractically tedious, further work on this line was dropped.

Frankel and Goldberg (3) list a solution for the boundary flux as follows:

$$\varphi_{(0)} = \sqrt{\frac{1}{2}\left(\frac{\Sigma_t}{\Sigma[1-\varkappa^2]} - 1\right)}$$

where the asymptotic flux goes as the hyperbolic sine vanishing at an "extrapolated" boundary thus:

$$\varphi_{a(z)} = \sinh \varkappa(z + z_0)$$

The extrapolation distance is given by:

$$z_0 = \frac{1}{\pi}\int_0^1 \frac{1}{1-\varkappa^2 s^2} \tan^{-1}\left(\frac{\pi/2}{\tanh^{-1} s - \Sigma/s\Sigma_t}\right) ds$$

The characteristic equation of the system relates $\varkappa$ to $\frac{\Sigma_t}{\Sigma}$, so the boundary flux may be expressed as a function of $\varkappa$ alone:

$$2\varphi_{(0)}^2 = \frac{\Sigma_t}{\Sigma(1-\varkappa^2)} - 1$$

$$\frac{\Sigma}{\Sigma_t}(1-\varkappa^2) = \frac{1}{1+2\varphi_{(0)}^2}$$

$$(1-\varkappa^2)\left(1 + \frac{\varkappa^2}{3} + \frac{\varkappa^4}{5} + \cdots\right) = \frac{1}{1+2\varphi_{(0)}^2}$$

$$\frac{2\varkappa^2}{3} + \frac{2\varkappa^4}{15} + \frac{2\varkappa^6}{35} + \cdots \frac{2\varkappa^{2n}}{(2n+1)(2n-1)} = 1 - \frac{1}{1+2\varphi_{(0)}^2}$$

$$\varkappa^2 + \frac{\varkappa^4}{5} + \frac{\varkappa^6}{7} + \cdots \frac{\varkappa^{2n}}{2n+1} = \frac{3\varphi_{(0)}^2}{1+2\varphi_{(0)}^2}$$

The procedure is as follows:

1. The extrapolation distance is computed by Simpson's Rule for a few values of $\varkappa$ in the neighborhood of 0.15 - 0.20 as indicated by the numerical solution, and plotted against $\varkappa$.
2. Selecting a value of $\varkappa$ and the corresponding z_0, the experimental boundary flux is normalized to go as $\sinh \varkappa (z + z_0)$ at large argument. This new normalization is obtained by halving that flux which was normalized to go asymptotically as $e^{\varkappa z}$ and multiplying by $e^{\varkappa z_0}$. The result is $\varphi_{(0)}$.
3. Insert the $\varphi_{(0)}$ in the series equation and solve by trial for $\varkappa$.
4. Using the computed values of $\varkappa$, return to stage (2) and iterate the process. Convergence is rapid.

The described process yielded $\Sigma = 2.10 \pm 0.05$ cm^{-1}.

CHAPTER III

EXPERIMENTAL PROCEDURE

The medium in which the experiment was conducted was the approximately 6' x 6' x 6' water tank which is mounted on the thermal column of the Oak Ridge Graphite Reactor. A current of thermal neutrons passes upward through the tank after filtering through the graphite column below. The water content is ion-exchange demineralized, and its nuclear properties are substantially those of distilled water.

A disk of aluminum, faced with .020 inch cadmium, and approximately 10" in diameter, carried on aluminum legs about 10" long, was lowered with a rod to a reproducible central location on the tank bottom. A foil holder of aluminum and lucite, fastened to the cadmium face was provided with adjustable mountings for positioning foils along the central normal to the plane. A foil was also cemented to the center of the cadmium plane for each exposure. The foil mountings were of lucite of minimum section consistent with stiffness, and a film of paraffin was employed as an adhesive to mount the foils, thus introducing no non-hydrogenous material in the immediate vicinity of the foils. The equipment is shown as Fig. (3).

Indium foils were used, weighing 25 milli-grams nominal, cut from 50 mg/cm^2 stock. These were cleaned of the adhesive wax after each use, weighed and allowed to decay for at least 48 hours before re-use.

Foil counting was done with an end mica-window Geiger-Mueller counter, connected through a plate-loaded pre-amplifier stage (of gain $\sim$ 12) to a scale of 64. Counter and pre-amplifier were enclosed in a 2" lead shield, which reduced background to a negligible fraction of the foil activity. Sufficient counts were obtained in each counting run to reduce statistical

fluctuation to a negligible level. A number of determinations of counter resolving time were made by following the decay of 54 min indium 116 over about 5 hours. An average value of 240 μsec. was obtained by solving the following:

$$\frac{A_1}{1 - N_1 \tau} = \frac{A_2}{1 - N_2 \tau}$$

where A = extrapolated activity

N = mean counting rate, sec^{-1}

τ = resolving time, sec.

A correction factor $1/1-N\tau$ was plotted against counting rate and applied to all counting runs to correct for coincidence losses.

For exposure, the foil holders (after mounting the foils) were adjusted approximately to position with respect to the cadmium plane using a common scale. A vernier height gauge was then used to determine the exact foil position (estimated probable error $\pm$ .05 mm.). The plane and foil holder assembly was then lowered quickly to the tank bottom and exposed for times ranging from 5 to 15 minutes depending on foil position to obtain reasonable counting rates. No attempt was made to measure either exposure or foil "cooling" times accurately since one foil always and two foils usually were exposed at fixed positions to monitor the activity of the variable foil. The positions at x = 0 and x $\cong$ 5.18 cm. are the monitor positions and data at these points represents an average of about 15 measurements. In addition to the exposures made with axial foils, two exposures were made with foils set in a plane parallel to the cadmium to demonstrate that the geometry was actually one dimensional. A plot of the diametral variation of flux appears as Fig. (6). The maximum deviation from the axial flux amounts to about

5% reduction at 8 cm. radius. This is considered satisfactory. To test the flux for fast components, a cadmium difference on Indium was taken. The ratio of activity in Cd. to activity in the "shadow" of the cadmium envelope (a most conservative condition) exceeded 5,000 - therefore foil activation due to the 1.44 volt resonance may be safely neglected.

To analyze the data by the numerical method, it was first plotted against the coordinate x in cms. on semi-log paper and the fair curve drawn by eye. A clearly exponential branch was obtained beginning at $x \sim 4.8$ cm. The decay constant k of the exponential was solved by

$$k = \frac{\ln \frac{\varphi(a)}{\varphi(b)}}{a - b}$$

and fixed at $k = 0.375$. The scale of the values of $\varphi(x)$ was then adjusted so that φ (asymptotic) $= e^{0.375x}$. A trial value of Σ was then selected, and the data plotted, faired and tabulated as a function of z in mean path measure. The eigenvalue $\frac{\Sigma_t}{2\Sigma}$ was computed, the $E_1(|m\Delta z|)$ tabulated on a strip for $\Delta z = .2$, and numerical iteration of the equation carried out until it was obvious that the solution near the plane at $z = 0$ would not fit the data. The trial was then terminated and another trial made for a different value of Σ.

As the solutions were improved it became clear that a correction was necessary for the remainder contributed by the terms beyond the last tabular value of the E_1. The correction was inserted by computing the remainder with respect to a proper exponential function and dividing by the value of this function at the first untabulated term of the E_1. This number is then used to terminate the E_1 tabulation. Since the last tabulated value of the E_1 was for $m\Delta z = 7.4$ one obtains:

$$e^{-7.6\varkappa}\int_{7.5}^{\infty} e^{\varkappa z}\, E_1(z)\, dz$$

which may be integrated by writing the E_1 as an integral, then inverting the order of integration to yield

$$\frac{1}{\varkappa}\, e^{-.1\varkappa}\left\{-E_1(7.5) + \frac{1}{\varkappa}\, e^{-7.5\varkappa}\, E_1(7.5-7.5\varkappa)\right\}$$

which must be computed individually for each value of Σ .

Iteration was carried out by computing only every fifth term of the trial function, then interpolating the new function by making the first differences regular. The final integration was done in detail in the region close to the black boundary.

Plots of the flux as a function of distance from the black boundary appear as Fig. (4) and (5). The curves were obtained by using the Le Caine results to interpolate the data near the boundary, and the numerically iterated function in the region more than 0.5 cm. from the boundary. The latter process is considered reasonable since the solutions in this region were invariant to changes in the integrating scheme, they are constrained by the approach to the asymptotic function, and they fit the data quite well.

Desirable extensions to the analysis might include:

(1) Computation of the Wiener-Hopf solution for perhaps 15 or 20 points to firm up confidence in the fit.

(2) Extensive analysis of the numerical iteration method to establish the level of computing detail necessary to yield accurate solutions using the true values of the parameters.

Both propositions require computing machine service to reduce program time to a practical value.

UNCLASSIFIED
DWG. 10140

FIG. I
VELOCITY DIAGRAM FOR TWO BODY COLLISION

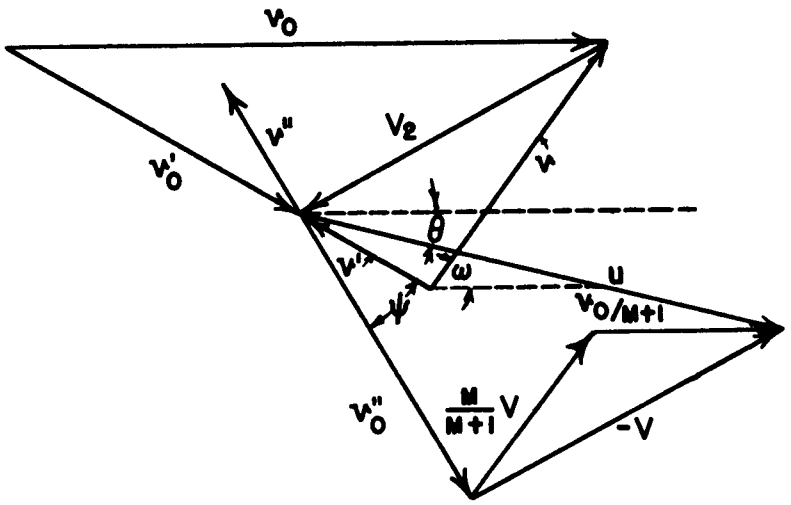

UNCLASSIFIED
DWG. 10141

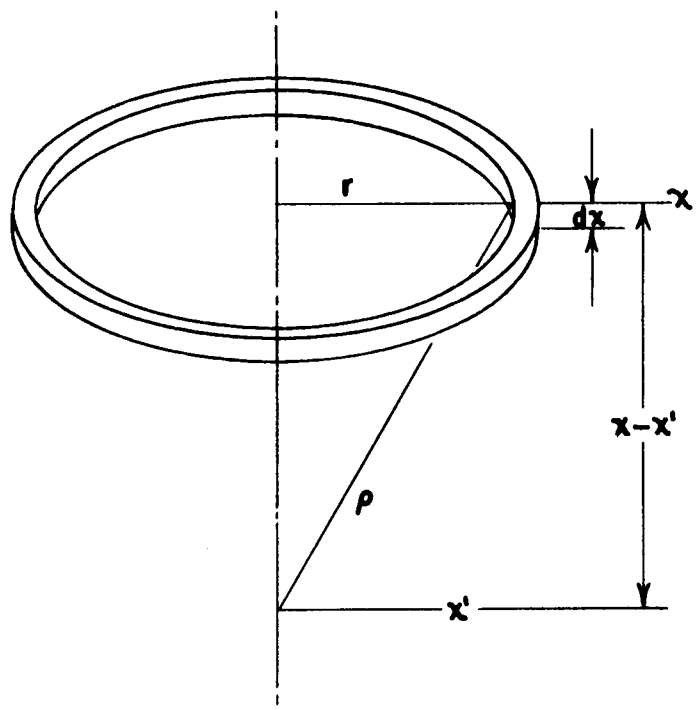

FIG. 2

INTEGRATION FOR PLANE KERNEL - TRANSPORT EQUATION

UNCLASSIFIED
DWG. 10144

FIG. 3

FOIL MOUNT AND CADMIUM PLANE ASSEMBLY

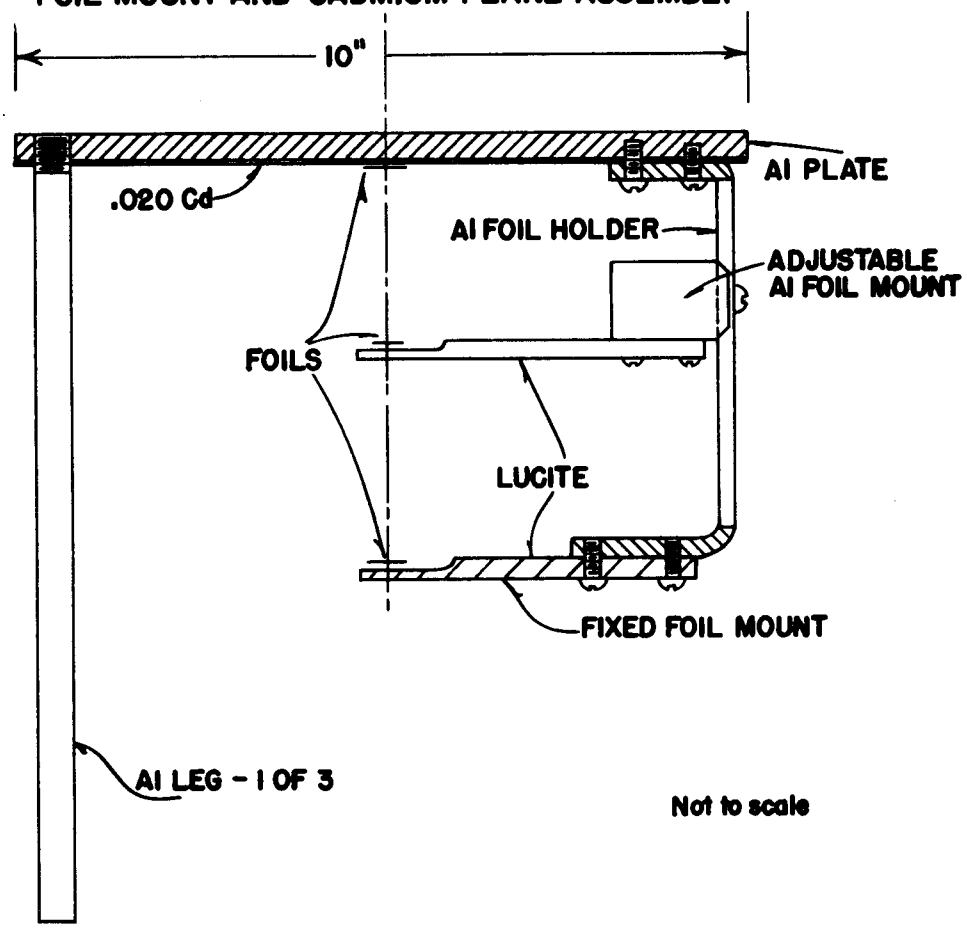

UNCLASSIFIED
DWG. 10142

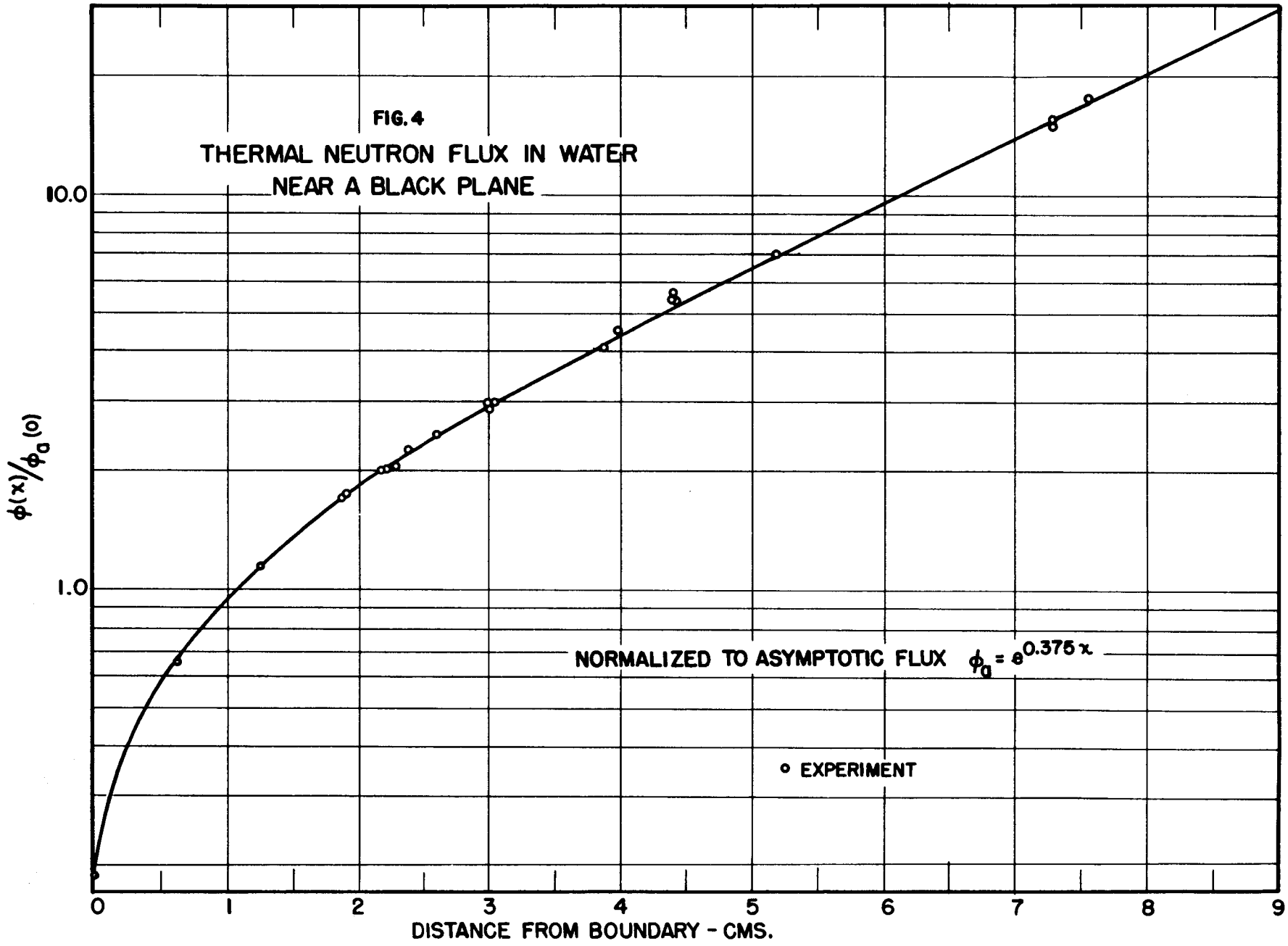

UNCLASSIFIED
DWG.10143

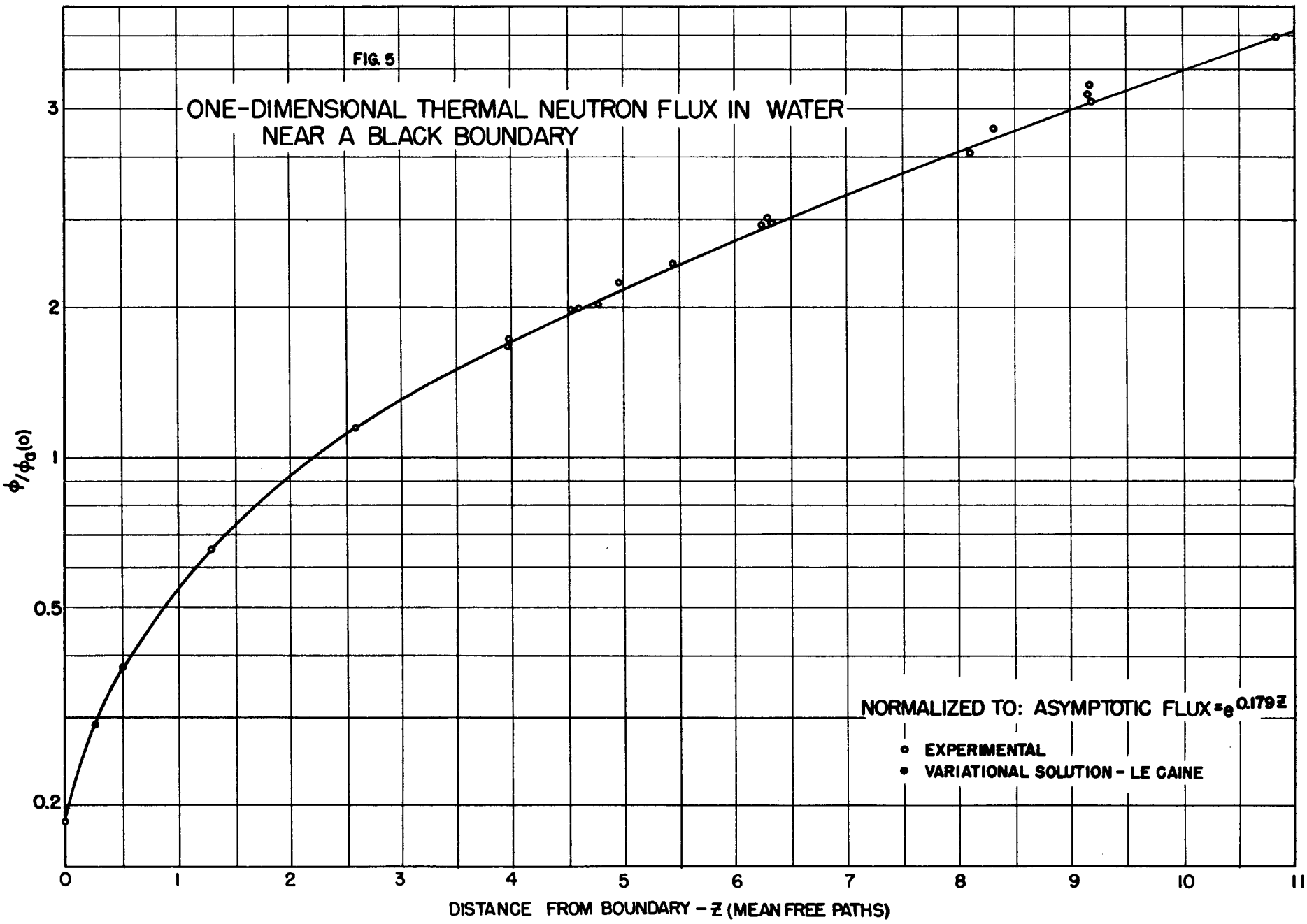

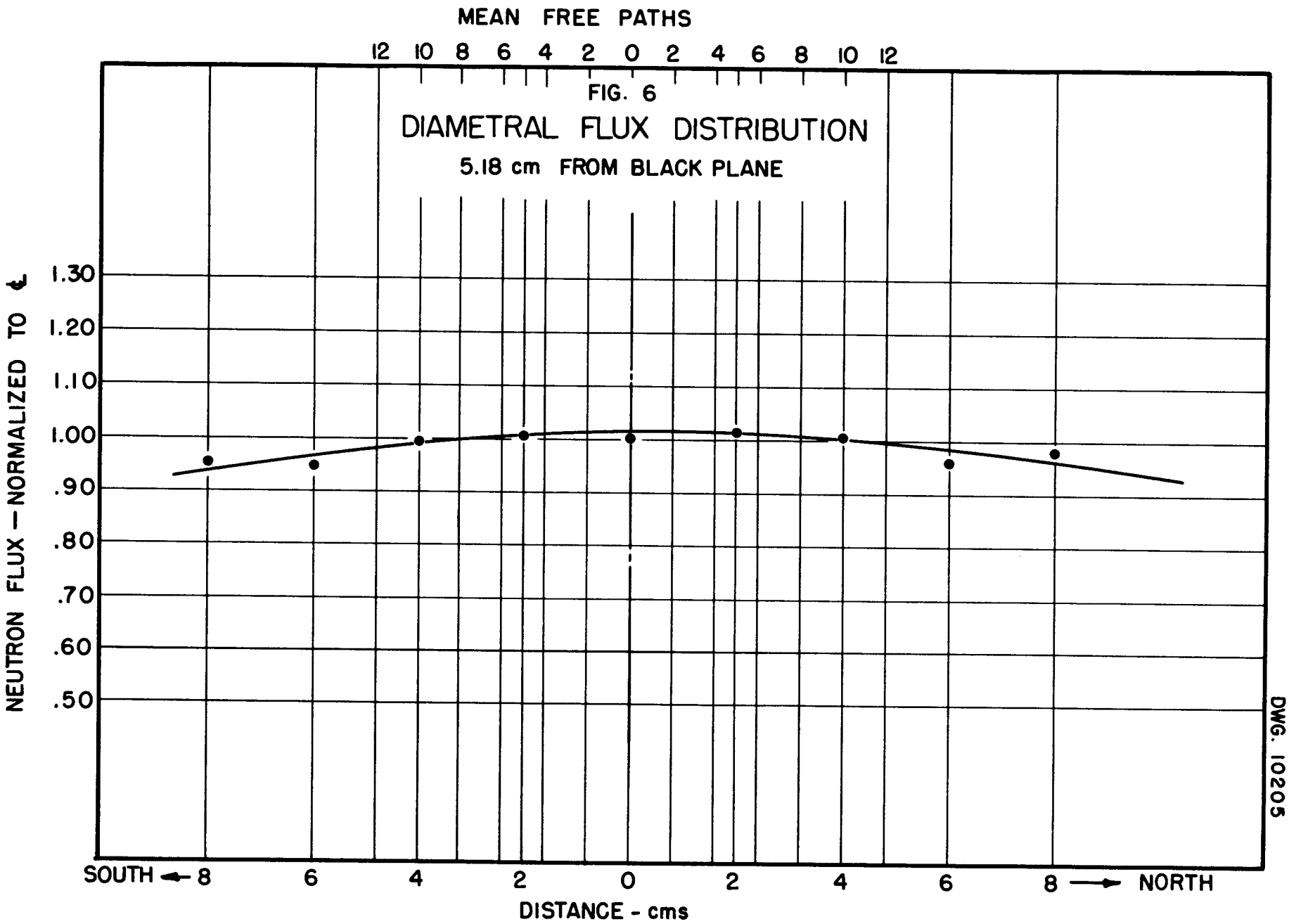

UNCLASSIFIED
DWG. 10205

BIBLIOGRAPHY

1. *The Slow Neutron Cross Section of Water as a Function of Energy. R. F. Bacher, C. P. Baker, M. G. Holloway and B. D. McDaniel. MDDC-512.

2. *Neutron Physics, J. G. Beckerley (A Revision of Halpern's notes on E. Fermi's 1945 Lectures) AECD-2664.

3. *The Mathematical Development of the End-Point Method. S. F. Frankel and S. Goldberg. AECD-2056.

4. *Methods of Treatment of Displacement Integral Equations. S. F. Frankel and E. C. Nelson. LA-53 (Secret).

5. On the Scattering of Thermal Neutrons. F. Joliot. Comptes Rendus Vol. 228 p. 245-6.

6. Neutron Flux Near a Black Plane. J. LeCaine, Canadian Journal of Research 28-3A p. 242.

7. *Slow Neutron Velocity Spectrometer Studies. E. Melkonian. AECD-2675.

8. On the Decrease of Neutron Density at a Boundary. H. Raether, Zeitschrift für Physik. Vol. 125 p. 269-273.

9. Vibrational Spectra and Structure of Polyatomic Molecules, Ta-You Wu Publ. J. W. Edwards, Ann Arbor, 1946.

*AEC Publications.

APPENDIX I

EXPERIMENTAL DATA -

COMPUTATION OF ACTIVITIES

Foil Inventory

Exposure Date + Setting in inches

Foil No.	Wt. mg.	Factor							
1	24.9	1.004	8/26 Cont.	8/29 Cont	8/30 2.195	9/1 2.040	9/6 Cont	9/8 2.023	
2	24.35	1.027	6/13 Cont	8/26 Cont.	8/29 Cont	8/30 2.195	9/1 2.040	9/6 1.729	9/8 2.862
3	24.3	1.029	6/13 0.490	8/26 2.026	8/29 Cont.	8/30 2.195	9/1 2.040	9/6 2.032	
4	23.5	1.064	6/13 2.043	8/26 0.866	8/29 1.192	8/30 2.195	9/1 2.040	9/7 1.729	
5	25.2	0.992	6/13 Cont.	8/26 Cont	8/29 2.043	8/30 2.195	9/1 2.040	9/6 0.934	9/8 Cont.
6	23.7	1.055	6/13 0.748	8/26 0.866	8/30 Cont.	9/1 2.040	9/6 2.030	9/8 0.900	
7	24.9	1.004	6/13 2.043	8/26 2.043	8/29 Cont	9/1 2.040	9/6 2.974	9/8 2.864	
8	22.4	1.116	8/27 0.244	8/29 1.025	9/1 2.040	9/6 Cont	9/7 2.020		
9	24.5	1.020	8/27 2043	8/29 2.040	8/31 Cont	9/1 2.040	9/7 Cont.		
10	23.2	1.078	8/27 Cont	8/30 0.854	8/31 1.567	9/1 0.748	9/2 0.490	9/7 1.178	
11	22.9	1.092	8/30 2.036	8/31 2.036	9/1 1.721	9/6 2.023	9/8 2.023		
12	23.35	1.071	9/1 2.030	9/2 Cont.	9/6 1.524	9/8 1.185			
13	24.9	1.004	9/1 Cont.	9/7 2.020					
14	23.7	1.055	9/1 2.038	9/2 2.030	9/7 Cont.				

Date	Foil	Setting cm.	Exposure Data	Delay Time min	Counting Time min	Counts/14 Counts	Background	Coincidence Correction	Net Counts	1/n	1/1-n	Relative Activity	Average Activity	Weight Factor	25 ma. Activity	Normal Factor	Normal Activity	Remarks	Z Set	Plot
6/13	U 2	.005		0	15	584.9	7.5	1.0068	580.0	1.—	5.7097	2170	2165	1.027	2223	640656	.142	Background = .5/min.		
	U 3	1.245	E-30	83	15	797.4	7.5	1.0139	803.0	2.9020	5.7097	13305	13221	1.029	13604	$\times 10^{-4}$	.872		2.60 3.11	1.150
	U 4	5.189	C-25.5	127	15	2575.2	7.5	1.0460	2686.2	5.1048	5.7097	78294	77928	1.064	82915		5.312	T_{water} = 71°F		
	U 2			24	50	773.6	25.0	1.0041	751.8	1.3608	2.1112	2160							10.84 12.97	7.007
	D 3			107	15	584.1	7.5	1.0105	582.6	3.9490	5.7097	13136								
	D 4			145	19	2530.1	9.5	1.0353	2609.9	6.4316	4.6206	77561								
6/13	U 5	.005		0	16	464.0	8.0	1.0077	459.6	1.—	5.3862	2475	2475	0.992	2455	575753	.141			
	U 6	1.900	E 30.5	37	15	2219.9	7.5	1.0395	2300.1	1.6079	5.7097	21116	20950	1.055	22102		1.273		3.97 4.75	1.679
	U 7	5.189	C 20.3	73	15	5728.0	7.5	1.1082	6340.3	2.5524	5.7097	92400	91911	1.004	92279		5.312			
	D 5			19	15	324.1	7.5	1.0059	318.5	1.2762	5.7097	2321								
	D 6			55	15	1750.0	7.5	1.0310	1796.8	2.0258	5.7097	20783								
	D 7			90	15	4650.1	7.5	1.0862	5043.4	3.1748	5.7097	91422								
8/26	U 2	.005		0	21	312.4	9.5	1.0040	304.1	1.—	4.2322	1287	1359	1.027	1396	1.023053	.143	U Standard (1) 92.8/min., (2) 92.3, (3) 91.9		
	U 6	2.200		50	10	880.2	4.5	1.0231	896.0	1.8999	8.3012	14131	14096	1.055	14871		1.512	Background = .45/min.	4.60 5.50	1.995
	U 7	5.189	E-15	72	5	1192.0	2.3	1.0645	1266.6	2.5198	16.086	51340	51716	1.004	51723		5.312			
	D 2			22	27	311.4	12.2	1.0031	300.2	1.3263	3.4142	1359								
	D 6		C-10	61	10	763.3	4.5	1.0201	774.1	2.1880	8.3012	14060						T_w = 68°F		
	D 7			79	5	1110.5	2.3	1.0599	1174.7	2.7567	16.086	52091								
8/27	D 10	.005		0	25	359.6	11.2	1.0039	349.8	1.—	3.6429	1274	1345	1.078	1450	.973054	.141	U Std. (1) 92.3, (2) 91.2	1.30 1.55	0.652
	D 8	.620		63	15	360.0	6.8	1.0063	355.5	2.2449	5.7097	4557	4553	1.116	5081		.494	Background = .43/min.		
	D 9	5.189	E-16	100	6	1051.0	2.7	1.0468	1097.5	3.6096	13.491	53445	53521	1.020	54591		5.312			
	U 10		C-16	26	36	371.6	16.2	1.0028	356.4	1.3962	2.7024	1345								
	U 8			79	20	380.7	9.0	1.0051	373.6	2.7567	4.4166	4549						T_w = 70°F		
	U 9			107	6	967.0	2.7	1.0431	1006.0	3.9490	13.4910	53596								
	D 1	.005		0	16	253.0	7.2	1.0042	246.9	1.—	5.3862	1330	1355		1360					
8/29	D 2	.005		36	20	192.6	9.0	1.0028	184.1	1.5874	4.4166	1291	1379	1.004	1355	1.020047	.141	Centered	U Std (1) 92.0	
	D 3	.005		82	28	150.1	12.6	1.0013	137.7	2.8650	3.3122	1307	1328	1.027	1364			4 cm. Off Center		
	D 4	3.028		164	10	304.6	4.5	1.0081	302.6	8.2080	8.3012	20618	1362	1.029	1401			4 cm. Off Center		
	D 5	5.189	E-15	175	6	404.1	2.7	1.0180	413.8	9.4528	13.491	52771	20786	1.064	22116		2.256		6.33 7.57	2.976
	U 1		C-15	17	18	236.0	8.1	1.0035	228.7	1.2439	4.8473	1379	52923	0.984	52076		5.312			
	U 2			57	24	184.3	10.8	1.0027	174.0	2.0785	3.7717	1364						T_w = 71°F		
	U 3			111	52	189.2	23.4	1.0011	166.0	4.1570	2.0534	1417								
	U 4			182	15	357.4	6.8	1.0063	354.9	10.340	5.7097	20953								
	U 5			199	15	720.3	6.8	1.0126	722.6	12.864	5.7097	53075								
8/29	7	.005		0	15	271.3	6.8	1.0049	265.8	1.—	5.7097	1518	1582	1.004	1588	.88245	.140			
	8	2.604	E 16	36	5	714.6	2.3	1.0381	739.5	1.5874	16.086	18883	18893	1.116	21085		1.860		5.44 6.51	2.454
	9	5.189	C 8	87	4	910.6	1.8	1.0616	964.9	3.0549	19.981	58897	59016	1.020	60196		5.312			
	7			16	18	272.7	8.1	1.0041	265.7	1.2280	4.8473	1582						T_w = 72°F		
	8			42	5	664.3	2.3	1.0353	685.4	1.7145	16.086	18903								
	9			93	4	850.2	1.8	1.0572	897.0	3.2994	19.981	59135								

Date	Foil	Setting	Exposure	T_2	T_3	Counts	Bckgrd.	1/M	Net Count	1/n	1/1-n	Activity	Average	Wt. Factor	25mg. Act.	Norm. Factor	Normal Activity		Set	Plot
8/30	D 6	.005		0	15	272.3	6.8	1.0048	266.8	1.—	5.7097	1523	1623	1.055	1712	.804064	.138	Background = .45/min; USfd (1) 91.4, (2) 92.3		
	D 10	2.169		37	5	654.5	2.3	1.0348	674.6	1.6079	16.086	17448	17382	1.078	18738		1.507		4.53 5.42	1.988
	D 11	5.171	E-15 C-9	138	6	739.5	2.7	1.0327	761.0	5.8789	13.491	60357	60366	1.092	65920		5.300			
	U 6			16	20	306.9	9.0	1.0041	299.2	1.2280	4.4166	1623						$T_W = 72°F$		
	U 10			43	6	718.9	2.7	1.0318	739.1	1.7366	13.491	17316								
	U 11			145	6	678.2	2.7	1.0300	695.8	6.4316	13.491	60374								
8/31	9	.005		0	20	225.6	9.0	1.0030	217.3	1.—	4.4166	960	1005	1.020	1025	1.388452	.142			
	10	3.980		52	5	702.3	2.3	1.0372	726.1	1.9493	16.086	22768	22953	1.078	24743		3.435		8.32 9.95	4.531
	11	5.171	E-11 C-19	68	5	867.1	2.3	1.0463	904.9	2.3937	16.086	34843	34956	1.092	38172		5.300			
	9			21	30	258.3	13.5	1.0023	245.4	1.3394	3.1289	1005						$T_W = 76°F$		
	10			58	7	915.7	3.2	1.0348	944.4	2.1054	11.637	23138								
	11			74	5	810.5	2.3	1.0432	843.2	2.5854	16.086	35068								
9/6	U 1	.005		0	21	486.6	9.5	1.0062	480.1	1.—	4.2322	2032	2032	1.004	2040	1.019307	.208			
	D 1		E-15 C-3	22	18	310.1	8.1	1.0046	303.4	1.3263	4.8473	1951								
	U 2	4.392		49	7	1747.8	3.2	1.0682	1863.8	1.8757	11.637	40682	40506	1.027	41600		4.240		9.18 10.98	5.593
	D 2			57	6	1358.1	2.7	1.0610	1438.2	2.0785	13.491	40329						$T_W = 74°F$		
	U 3	5.156		67	8	1955.7	3.6	1.0666	2082.3	2.3632	10.247	50424	50435	1.029	51898		5.290			
	D 3			76	10	2168.5	4.5	1.0585	2290.9	2.6526	8.3012	50445								
	U 2			156	53	2682.3	23.9	1.0132	2693.8	7.4070	2.0262	40429								
	U 3			211	9	370.7	4.1	1.0108	370.6	14.9992	9.1650	50946								
9/1	D 11	4.371		0	6	1842.2	2.7	1.0852	1996.5	1.—	13.491	26935	26980	1.092	29462	1.38232	4.073	USfd. = 91.4/min	9.14 10.93	5.373
	D 12	5.156		31	4	1116.4	1.8	1.0770	1200.6	1.4887	19.981	35713	35732	1.071	38269		5.290			
	U 11		E-12 C-25	10	5	1375.6	2.3	1.0758	1477.6	1.1370	16.086	27025								
	U 12			36	5	1308.8	2.3	1.0715	1400.1	1.5874	16.086	35751								
	U 11			18	11	1151.1	5.0	1.0276	1177.9	1.2599	7.5941	11270						Shelf #2 - Factor = .4191		
9/1	U 13	.005		0	31	450.0	14.0	1.0040	457.8	1.—	3.0462	1334	1334	1.014	1339	1.036613	.139			
	U 10	1.900	E-12 C-5	34	5	461.1	2.3	1.0243	470.0	1.5472	16.086	11697	11674	1.078	12585		1.305	$T_W = 75°F$	3.97 4.75	1.721
	U 14	5.177		47	5	1526.5	2.3	1.0844	1653.0	1.8281	16.086	48609	48463	1.055	51128		5.300			
	D 10			40	6	508.2	2.7	1.0223	516.8	1.6710	13.491	11650								
	D 14			53	5	1409.0	2.3	1.0779	1516.5	1.9745	16.086	48167								
	D 14			63	5	1261.6	2.3	1.0689	1346.2	2.2449	16.086	48613								
9/6	U 5	2.372		0	10	354.0	4.5	1.0093	352.8	1.—	8.3012	2929	2929	0.992	2906	.584474	1.704		4.96 5.93	2.248
	U 6	5.156	E-5 C-7½	11	8	712.0	3.6	1.0234	725.1	1.1517	10.247	8557	8550	1.055	9020	$\times 10^{-3}$	5.290			
	U 7	7.554		20	5	1013.6	2.3	1.0547	1066.7	1.2927	16.086	22181	22069	1.004	22157		12.995	$T_W = 74°F$	15.79 18.89	17.142
	U 6			93	11	343.1	5.0	1.0082	340.9	3.2994	7.5941	8542								
	U 7			105	8	550.3	3.6	1.0182	556.7	3.8489	10.247	21956								
	U 7			258	30	271.8	13.5	1.0024	259.0	27.432	3.1289	22230								

Date	Foil	Set.	Exposed	T_2	T_3	Counts	Bckgd.	1/n	Net Count	1/n	1/1-n	Activity	Average	Wt. Fact.	25mg Activity	Norm Factor	Normal Activity	Set	Plot
9/6	U 8	.005	E-10 C-5½	0	42	431.5	18.9	1.0028	413.8	1.—	2.3996	993	993	1.116	1108	1.278024	.142		
	U 12	3.871		43	15	2212.5	6.8	1.0393	2292.7	1.7366	5.7097	22733	22640	1.071	24247		3.099	8.09	9.68 4.088
	D 12			59	10	1237.5	4.5	1.0328	1273.6	2.1326	8.3012	22547							
	U 11	5.156		72	22	3554.5	9.9	1.0431	3697.8	2.5198	4.0647	37874	37905	1.092	41392		5.290		
	D 11			95	26	3094.1	11.7	1.0315	3179.9	3.3852	3.5241	37936							
9/7	U 9	.005	E-10 C-4½	0	25	319.6	11.2	1.0034	309.5	1.—	3.6429	1127	1127	1.020	1150	1.231206	.142	Backgrd. = .42/min.	
	D 9			26	33	281.6	14.8	1.0023	267.4	1.3962	2.8960	1081						USTd. (1) 92.2	
	D 4	4.391		64	8	1229.1	3.6	1.0410	1275.9	2.2739	10.247	29729	29728	1.064	31631		3.894	9.18	10.98 5.137
	U 4			73	10	1358.6	4.5	1.0360	1403.0	2.5524	8.3012	29727							
	D 13	5.156		85	5	841.2	2.3	1.0450	876.8	2.9774	16.086	41994	42795	1.004	42966		5.290	T_w = 76°F	
	U 13			96	54	6225.5	24.3	1.0304	6390.5	3.4290	2.000	43826							
	U 13			347	20	120.9	9.0	1.0017	112.1	85.971	4.4166	42564							
9/7	U 14	.005	E-16 C-6½	0	41	659.5	18.5	1.0043	643.8	1.—	2.4438	1573	1573	1.055	1660	.825585	.137		
	U 14			50	11	113.7	4.9	1.0029	109.1	1.8999	7.5941	1574							
	D 10	2.992		43	5	847.7	2.3	1.0449	883.5	1.7366	16.0860	24681	24815	1.078	26751		2.209	6.25	7.48 2.914
	U 10			63	10	1298.5	4.5	1.0345	1338.8	2.2449	8.3012	24949							
	D 8	5.130		74	9	2250.6	4.0	1.0684	2400.5	2.5854	9.1650	56880	56764	1.116	63349		5.230		
	U 8			84	15	3198.6	6.8	1.0573	3375.1	2.9395	5.7097	56647							
9/8	D 12	3.009	E-11 C-12	0	6	1108.3	2.7	1.0495	1160.5	1.—	13.491	15656	15646	1.071	16757	1.280328	2.145	6.29	7.52
	U 12			28	16	1969.5	7.2	1.0326	2026.5	1.4325	5.3862	15636						USTd (1) 91.8, (2) 91.9	2.830
	D 11	5.138		46	12	2789.7	5.4	1.0629	2960.0	1.8048	7.0050	37422	37479	1.092	40927		5.240	T_w = 75°F	
	U 11			60	8	1612.0	3.6	1.0542	1695.8	2.1601	10.247	37536							
	D 7	7.275		123	15	3005.1	6.8	1.0539	3160.3	4.8493	5.7097	87503	87458	1.004	87808		11.242	15.20	18.19 14.830
	U 7			139	16	2617.8	7.2	1.0438	2725.3	5.9549	5.3862	87412							
	U 12			71	50	2938.0	22.5	1.0154	2960.7	2.4877	2.1112	15550							
	U 7			334	11	160.7	5.0	1.0040	156.3	72.748	7.5941	86349							
9/8	U 5	.005	E-12 C-7	0	36	480.8	16.2	1.0036	466.3	1.—	2.7024	1260	1260	0.992	1250	1.118033	.140		
	D 6	2.286		37	11	1045.7	5.0	1.0251	1066.9	1.6079	7.5941	13027	13074	1.055	13793		1.542	4.78	5.72 2.034
	U 6			49	14	1132.9	6.3	1.0213	1150.7	1.8757	6.0795	13122							
	D 1	5.138		64	6	1428.3	2.7	1.0646	1517.9	2.2739	13.491	46565	46681	1.004	46868		5.240		
	U 1			71	5	1105.9	2.3	1.0595	1169.4	2.4877	16.086	46796							
	D 2	7.269		119	5	1280.8	2.3	1.0701	1368.3	4.6066	16.086	101393	101306	1.027	104041		11.632	15.19	18.17 15.344
	U 2			125	5	1190.1	2.3	1.0646	1264.7	4.9754	16.086	101219							

APPENDIX II

The flux is tabulated as a function of Z for two values of the total cross section. These are solutions corresponding (for $\Sigma = 2.3$) to the most elaborate numerical treatment, and (for $\Sigma = 2.1$) to the best reconciliation of Wiener-Hopf, variational, and numerical and experimental solutions.

Z	$\phi(\Sigma = 2.1)$	$\phi(\Sigma = 2.3)$	Z	$\phi(\Sigma = 2.1)$	$\phi(\Sigma = 2.3)$
0	1.86	1.86	4.2	18.00	16.45
0.2	2.71	2.70	4.4	18.90	17.20
0.4	3.44	3.45	4.6	19.80	18.00
0.6	4.15	4.14	4.8	20.75	18.80
0.8	4.84	4.80	5.0	21.75	19.70
1.0	5.52	5.44	5.2	22.75	20.60
1.2	6.20	6.07	5.4	23.80	21.50
1.4	6.88	6.69	5.6	24.90	22.40
1.6	7.57	7.30	5.8	26.00	23.25
1.8	8.29	7.93	6.0	27.10	24.20
2.0	9.04	8.59	6.2	28.20	25.20
2.2	9.84	9.25	6.4	29.50	26.20
2.4	10.64	9.93	6.6	30.70	27.25
2.6	11.49	10.60	6.8	32.00	28.30
2.8	12.30	11.30	7.0	33.40	29.45
3.0	13.05	12.00	7.2	34.80	30.55
3.2	13.85	12.75	7.4	36.10	31.75
3.4	14.65	13.50	7.6	37.60	33.00
3.6	15.45	14.25	7.8	39.10	34.20
3.8	16.30	14.95	8.0	40.80	35.50
4.0	17.15	15.70			